This is a “preproof” accepted article for *Mineralogical Magazine*.
This version may be subject to change during the production process.
10.1180/mgm.2024.57

Differential dissolving kinetics of trioctahedral lizardite, chlorite, and talc-water interface reaction in acid environment

Dingran Zhao [1,2], Hongjuan Sun [1,2,*], Tongjiang Peng [1,2], Li Zeng [1,2]

[1] Key Laboratory of Ministry of Education for Solid Waste Treatment and Resource Recycle, Southwest University of Science and Technology, Mianyang, Sichuan 621010, China

[2] Institute of Mineral Materials and Applications, Southwest University of Science and Technology, Mianyang, Sichuan 621010, China

Abstract: Based on the chemical properties of different two-dimensional structural units of layered silicate minerals and their reaction properties to acidic media, sulfuric acid solution-mineral leaching systems with pH values of 2.0, 4.0 and 6.0 were constructed to investigate the differential dissolution properties of lizardite, chlorite and talc and the chemical kinetic mechanism of mineral-water interface reaction. The results showed that the dissolution efficiency of Mg in lizardite is higher than that of chlorite and talc in acidic environments with pH values of 2.0, 4.0 and 6.0. The dissolution efficiency of Mg in chlorite is greater than that of talc in acidic environment with pH value of 2.0 and 4.0. Chlorite and talc have nearly identical Mg dissolution efficiencies at a pH of 6.0. This phenomenon is related to the defect site on the tetrahedral sheet of chlorite and is controlled by the change of the dissolution efficiency of Al. The dissolution rates of Mg and Si in lizardite, chlorite and talc decreased with the increase of reaction time in acidic medium with pH values of 2.0, 4.0 and 6.0, and there are

* Corresponding author at: Key Laboratory of Ministry of Education for Solid Waste Treatment and Resource Recycle, Southwest University of Science and Technology, Mianyang, Sichuan 621010, China.
E-mail address: sunhongjuan@swust.edu.cn (H. Sun).

https://doi.org/10.1180/mgm.2024.57 Published online by Cambridge University Press

two linear dissolution trends at different pH values. The dissolution efficiencies of Mg and Si in lizardite, chlorite and talc were simulated and predicted by establishing a Logistic model. It is found that the maximum dissolution efficiency of chlorite and talc as 2:1 type minerals are only 4.72% and 1.58%, which is much lower than that of 1:1 type lizardite. The research on the reaction mechanism and dissolution kinetics of lizardite, chlorite and talc not only help to deepen the understanding of the mineral-water interface interaction, but also reveals the different rules of Mg, Si and Al dissolution in different types of trioctahedral mineral-water interface reaction, and provides a crystal chemical basis for the ion migration and action mechanism of minerals.

Keywords: Lizardite, Chlorite, Talc, Differential dissolution, Chemical kinetics

Introduction

Phyllosilicate minerals play an important role in the physical and chemical processes of many natural systems, especially under the action of aqueous solution (the presence of water molecules), refining, component dissolution, exchange/adsorption, structural evolution and other processes are constantly occurring, which is very important to maintain the function of the Earth ecosystem (Sposito, 1989; Hao et al. 2019). Due to the development of human industrial production, industrial wastewater discharged from coal burning, oil burning, mining and processing, organic and inorganic chemical production, etc., leads to air pollution and acid rain, resulting in local water or soil acidity (Ren et al. 2023). This further increases the reaction rate and complexity of the reaction process at the mineral-water interface. Therefore, the reaction process and results of layered silicate minerals in acidic media should be fully understood.

A lot of basic research has been done on the weathering of phyllosilicate minerals (Stumm and

https://doi.org/10.1180/mgm.2024.57 Published online by Cambridge University Press

Wieland, 1990; Meng et al. 2016; Peng et al. 2016). Among them, the weathering of dioctahedral minerals such as kaolinite and montmorillonite is more studied (Amram and Ganor, 2005; Cappelli et al. 2018; Krupskaya et al. 2019; Lin et al. 2020). The reaction mechanism of trioctahedral minerals such as lizardite, chlorite, talc and vermiculite in acidic media has gradually attracted attention. The main results show that Mg^{2+} in different lizardite minerals has different dissolution characteristics, and the dissolution rate of Mg^{2+} is closely related to the crystal structure, chemical properties and microscopic morphology (Lacinska et al. 2016). In sulfuric acid solutions with different pH values, the dissolution rate and the sequence of ion release of chlorite are controlled by pH value, and the higher the concentration of H^{+}, the more favorable the preferential release of Fe^{3+} from the octahedron (Liao et al. 2021). When talc is reacted in a closed solution system at 25℃ and pH 5, it can be found that the dissolution rate of Mg in octahedral sheets is higher than that of Si in tetrahedral sheets, and the dissolution rate of talc is controlled by the degree of destruction of silica tetrahedral sheets (Lin and Cemency, 1981). With the in-depth study of talc in different pH ranges, it has been found that pH has little or no effect on the dissolution rate of talc (Jurinski and Rimstidt, 2001). After summarizing the dissolution process of stratified silicate minerals in different acidic media, it is found that it is difficult to compare the research results due to the different experimental conditions of the obtained data. Therefore, there is a lack of research on the chemical kinetics mechanism of mineral-water interface based on the different properties of different two-dimensional structural units of phyllosilicate minerals. Due to differences in composition and structure, dioctahedral minerals generally exhibit greater stability than trioctahedral minerals. Consequently, trioctahedral minerals demonstrate higher ion dissolution rates and migration abilities, leading to a more significant impact on the ecological environment. Therefore, this study selects trioctahedral minerals as the research

https://doi.org/10.1180/mgm.2024.57 Published online by Cambridge University Press

object.

Lizardite, chlorite and talc belong to the trioctahedral phyllosilicate minerals. Their structural layers are formed by the combination of silica tetrahedral sheet (Si_2O_5) (T) and octahedral sheet M- (O, OH) (O). Between the structural layers are interlayer domains with or without interlayer matter (Gazze et al. 2014; He et al. 2016). For example, lizardite (1:1 type, no interlayer, Fig. 1a), talc (2:1 type, no interlayer, Fig. 1b) and chlorite (2:1 type, interlayer, Fig. 1c), along the c-axis, the structural layers and interlayer domains form structural unit layers or crystal layers (Hegyesi et al. 2020). The minerals in different crystal layers have different composition, structure and chemical bond strength properties, so they have different chemical stability and dissolution kinetics, and the siloxane or hydroxyl base surface and corresponding edge (end surface) formed by them should have different chemical activities.

In this research, by constructing percolation systems with different pH values (ranging from 2 to 6) and simulating acid precipitation, leaching experiments were carried out on minerals, and an open mineral-water interface reaction environment was established to analyze the mineral filtrate residue and filtrate samples after leaching. In order to investigate the structural changes and the dissolution efficiency and dissolution rate of components in the mineral-water interfacial reaction of lizardite, chlorite and talc under different acidic environments, the kinetic model of Mg and Si dissolution in lizardite, chlorite and talc was established.

https://doi.org/10.1180/mgm.2024.57 Published online by Cambridge University Press

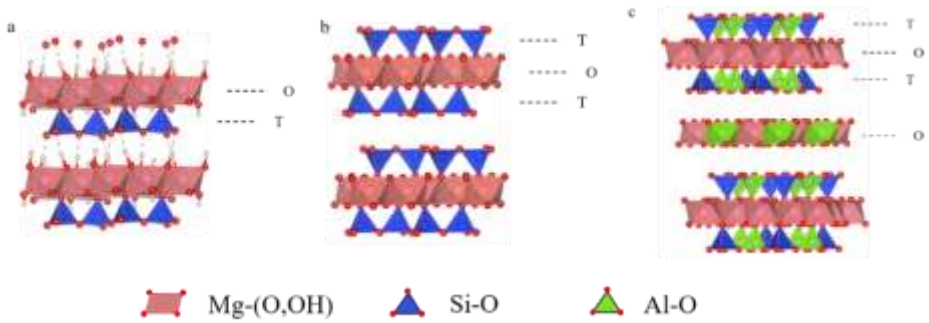

Fig. 1. Schematic diagram of crystal structure of lizardite (a), talc (b) and chlorite (c).

Materials and methods

Materials and reagents

Lizardite and chlorite were collected from Xiuyan County, North Wagou Xiuyu Mine, and talc was collected in Guilin Longsheng, Guangxi. The samples were crushed and ground (through 200 mesh screening). In order to minimize the influence of high-energy surface sites and fine particles generated during the grinding process, the samples were rinsed three times in ultrapure water (resistivity ≥ 18.2 mΩ cm) subsequent to ultrasonic bath. pH value was adjusted with a solution of sodium hydroxide (NaOH, 1%) and dilute sulfuric acid (H_2SO_4, 1%). All chemical reagents were analytical grade reagents, provided by Chengdu Kelong Chemical Ltd. All experiments were carried out in the leaching device, as shown in Fig. 2.

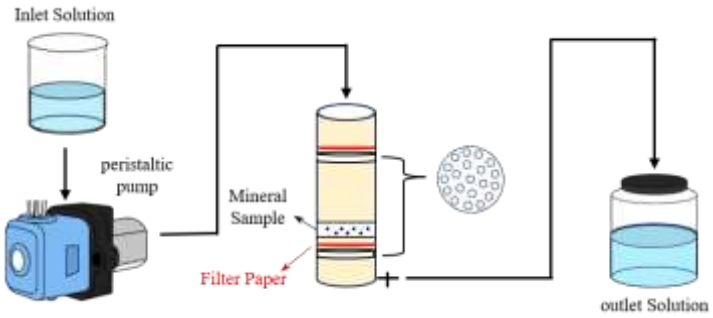

Fig. 2. Experimental apparatus used in the leaching process.

https://doi.org/10.1180/mgm.2024.57 Published online by Cambridge University Press

Experimental

At room temperature, samples of 1 g lizardite, chlorite, and talc minerals respectively were weighed and placed in the leachate (Fig. 2). The leaching method was used to replace the mixed flow reactor, which was closer to the natural system. In the leaching process, the pH value of the leaching solution is always kept constant to prevent the experimental error caused by the change of pH value when reacting with the mineral sample; Simultaneously, the solution will be transferred after a water interface interaction between air precipitation and mineral samples in their natural environment. Additionally, the reaction device will be built to release the filtrate after the reaction. The leaching solution used was sulfuric acid solution with pH values of 2.0, 4.0 and 6.0, respectively. In the leaching experiment, the flow rate of sulfuric acid solution with different pH values was set at 0.4 mL/min, and the duration of the experiment was 40 hours. The filtrate is collected in a closed glass bottle and analyzed every 4 hours for a total of 10 sample solutions. The sample solution is used for ICP analysis to calculate the concentrations of Mg, Si and Al in the solution. After the leaching experiment was completed, the solid mineral samples were washed 3 times with ultrapure water, dried at 60°C, and then ground for X-ray diffraction (XRD) test. The samples were labeled as Lz, Chl, and Tlc, for lizardite, chlorite and talc respectively.

Characterization

Chemical analysis of major elements was performed by X-ray fluorescence (XRF). Elements were analyzed using Axios series X-ray fluorescence spectrometer, equipped with an X-ray tube with a Rh anode and a maximum voltage/current of 60 kV/150 mA. The fundamental parameter method using Spectra plus software was used to quantify the elements.

https://doi.org/10.1180/mgm.2024.57 Published online by Cambridge University Press

The specific surface area of the lizardite, chlorite and talc were measured by the Brunauer–Emmett–Teller (BET) method, using 5-point N_2 adsorption isotherms, after degassing the sample for 60 min at 120 °C, using a McASAP 2460 (Norcross, Georgia, USA) instrument.

X-ray diffraction (XRD) was used to determine the mineralogical changes in the samples before and after the water-interface reaction. XRD data were obtained using a D/max-IIIA diffractometer manufactured by Rigaku (Tokyo, Japan). A copper target with a sum-tube voltage of 40 kV and a sum-tube current of 40 mA was accompanied by a slit system DS1/2(°). The powdered samples were analyzed between 3 and 80° of 2θ value. The step size was 0.02°2θ and the scan rate was 2 s/step.

The cation (Mg, Si) content in solution was measured by an inductively coupled plasma emission spectrometer (ThermoiCAP 6500, Waltham, Massachusetts, USA). Prior to each analysis, the ICP was calibrated ($r^2 > 0.999$) via serial dilution of certified standards (BDH Limited).

The average rate of dissolution of each ion in the mineral is calculated as follows:

$$r_i(\bar{t}) = \frac{Ci \times m_1}{t \times m_0 \times SSA \times \eta_i} \quad (1)$$

where C_i is the concentration of solute i (Mg, Si, Al, mmol/kg) in the sample recovered at time t; m_1 is the mass of the sample solution before sampling (in kg); t is the sample reaction time; m_0 is the initial mass of the mineral (in g); SSA (m^2/g) is the specific surface area of the mineral; and η_i is the stoichiometric coefficient of element i in the mineral.

Results and Discussion

Chemical analysis of raw minerals

The XRF analysis of the purified samples of lizardite (Lz), chlorite (Chl) and talc (Tlc) are

https://doi.org/10.1180/mgm.2024.57 Published online by Cambridge University Press

shown in Table 1. The typical structural layer of Lz is 0.44 nm thick and consists of tetrahedral and octahedral sheets (Wang et al. 2006; Evans et al. 2013). In the tetrahedral sheets, Si is replaced by Al and Fe, while in the octahedral sheets, Mg is replaced by Fe and a small amount of Cr, Ni, and Ti (Mellini and Zanazzi, 1987; Fuchs et al. 1998). Chl consists of a negatively charged tetrahedral-octahedral-tetrahedral (TOT) layer with a thickness of 0.66 nm and a positively charged interlayer octahedral sheet with a thickness of 0.22 nm (Brigatti et al. 2013). In the tetrahedral sheet, Al replaces Si, and in the octahedral sheet, Al and Fe replace Mg, and a small amount of Cr and Mn occupy the octahedral sheets (Barnhisel and Bertsch, 1989). Tlc is 2:1 type structure, where the tetrahedral sheet only contains Si, there is a small amount of Fe instead of Mg in the octahedral sheets (Douillard et al. 2007; Saldi et al. 2007). According to Table 1, the crystal chemical formulas of Lz, Chl and Tlc were calculated on the basis of (O) 11 and (O) 14 oxygen atoms:

Lz：$(Mg_{5.418}Fe_{0.402}Cr_{0.028}Ni_{0.02}Ti_{0.007})_{5.875}[(Si_{3.777}Al_{0.123}Fe_{0.1})_4O_{10}]\ (OH)_8$

Chl：$(Mg_{3.401}Fe_{1.105}Al_{0.956}Mn_{0.033}Cr_{0.007})_{5.502}\ [(Si_{2.586}Al_{1.414})_4O_{10}]\ (OH)_8$

Tlc：$(Mg_{2.987}Fe_{0.013})_3[Si_4O_{10}]\ (OH)_2$

Table 1

Chemical composition of Lz, Chl and Tlc samples (wt.%).

Sample	SiO_2	MgO	Fe_2O_3	Al_2O_3	K_2O	Cr_2O_3	BaO	NiO	SO_3	TiO_2	CaO	MnO	LOI.	Total
Lz	38.93	37.46	6.88	1.08	0.59	0.36	0.30	0.26	0.17	0.10	0.10	0.01	13.67	100.00
Chl	25.74	22.71	14.61	20.01	0.59	0.09	0.28	<0.01	0.11	4.48	0.42	0.39	10.44	100.00
Tlc	64.25	32.01	0.27	0.05	0.42	<0.01	0.20	<0.01	0.02	0.02	0.61	<0.01	2.03	100.00

Leaching based variations in mineral structure

XRD analysis

https://doi.org/10.1180/mgm.2024.57 Published online by Cambridge University Press

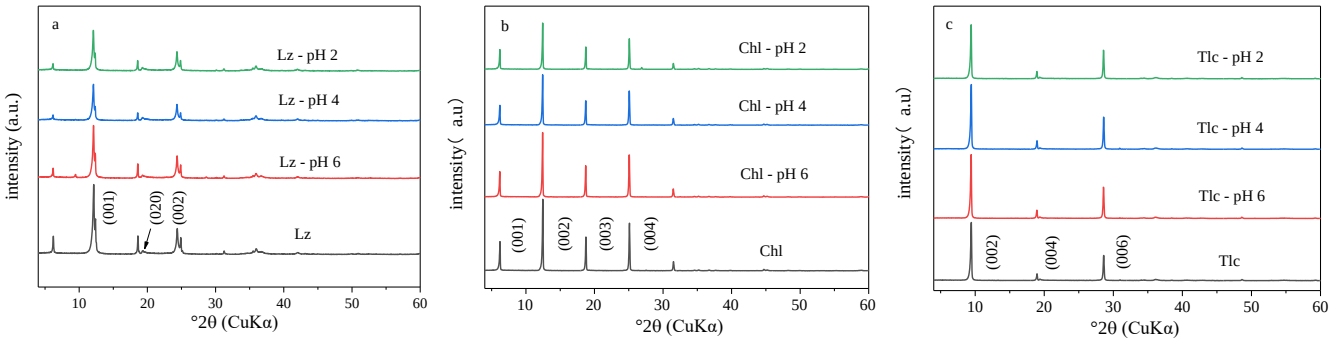

Fig. 3. XRD pattern of mineral samples with sulfuric acid solution at pH 2.0, 4.0 and 6.0 after leaching for 40 hours. a. Lz; b. Chl; c. Tlc.

According to Fig. 3, the diffraction peaks of the original Lz are d_{001} = 7.29Å, d_{110} = 4.76Å and d_{002} = 3.64Å, and contain a small amount of Chl (d_{001} = 14.1Å, d_{004} = 3.67Å). The diffraction peak of Chl is only found in Chl (d_{001}= 14.23Å, d_{002}= 7.11Å, d_{003}= 4.73Å, d_{004}= 3.55Å). The diffraction peaks of Tlc are d_{002}= 9.37Å, d_{004}= 4.67Å and d_{006}= 3.12Å. After being leached by sulfuric acid solutions with pH values of 2.0, 4.0 and 6.0 for 40 hours, the intensity of d_{00l} series diffraction peak decreases with the decrease of pH value of sulfuric acid solution. It shows that the crystal structure of Lz and Chl is further destroyed with the "attack" of H^+ in solution. After the Tlc samples were leached by sulfuric acid solution with different pH values for 40 hours, the diffraction peak intensity did not change significantly. Therefore, compared with Lz and Chl, Tlc is more stable, and the "attack" of H^+ in the solution will not cause obvious damage to the crystal structure of Tlc.

SEM analysis

https://doi.org/10.1180/mgm.2024.57 Published online by Cambridge University Press

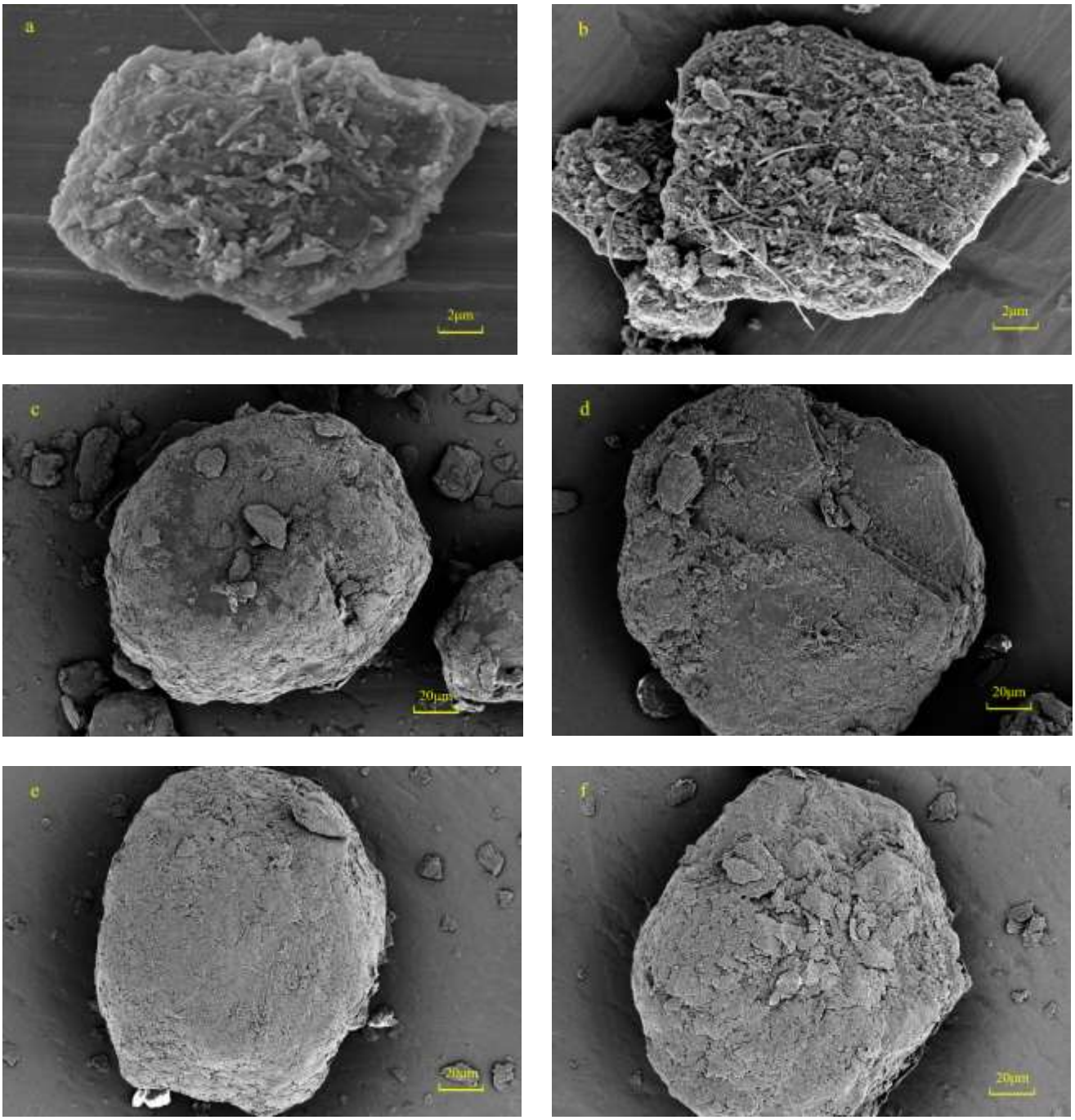

Fig.4 SEM images:(a) Lz original, (b) Lz in sulfuric acid solution with pH 2.0 (c) Chl original, (d) Chl in sulfuric acid solution with pH 2.0, (e) Tlc original, (f) Tlc in sulfuric acid solution with pH 2.0.

The Lz original sample (Fig. 4a) mainly presents lamellar micromorphology, with some small mineral particles and tubular chrysotile attached to the surface. After Lz reacts with sulfuric acid solution with pH of 2.0 for 40 h (Fig. 4b), the laminar main structure is retained, the outer surface is

https://doi.org/10.1180/mgm.2024.57 Published online by Cambridge University Press

corroded and forms erosion pits. The large layer structure is destroyed into small layers, and more small mineral particles and tubular chrysotile corroded by H^+ were adsorbed on the Lz surface. The original structure of Chl is relatively complete (Fig. 4c). After 40 h reaction with a pH of 2.0 sulfuric acid solution. Obvious erosion can be found on the surface of Chl, and clear lamellar structures can be seen from the edge of the destroyed mineral. This also indicates that the dissolution of Chl in acidic solution occurred at the grain edge, and at the cracks and structural defects (Ross, 1969; Kameda et al., 2009). For Tlc, after reaction for 24 h (Fig. 4f), the edge lamellae were attacked by H^+, the structure was destroyed and corroded, and part of the structure of Tlc collapsed. The Tlc surface undergoes corrosion, resulting in the formation of small flakes that adhere to the mineral surface.

Dissolution of Mg, Si and Al in minerals

Dissolution efficiencies of Mg, Si and Al

Table 2

Concentrations of Mg, Si and Al in solution after leaching Lz, Chl and Tlc in sulfuric acid medium with pH of 2.0, 4.0 and 6.0 for different time (mg/L).

Time	pH	Mg			Si			Al		
		Lz	Chl	Tlc	Lz	Chl	Tlc	Lz	Chl	Tlc
4h	2	33.05	12.83	13.46	2.76	4.21	0.49	-	6.91	-
8h	2	30.06	10.53	10.24	2.75	3.90	0.41	-	6.31	-
12h	2	26.68	9.17	8.07	2.47	3.67	0.34	-	5.81	-
16h	2	25.71	8.30	6.70	2.65	3.49	0.35	-	5.42	-
20h	2	23.44	7.34	5.47	2.43	3.25	0.30	-	4.86	-
24h	2	22.97	6.55	4.65	2.47	2.99	0.28	-	4.34	-
28h	2	21.95	5.95	4.04	2.36	2.79	0.26	-	3.97	-
32h	2	21.07	5.44	3.57	2.26	2.58	0.25	-	3.62	-
36h	2	20.36	5.05	3.21	2.18	2.42	0.24	-	3.36	-

https://doi.org/10.1180/mgm.2024.57 Published online by Cambridge University Press

40h	2	19.73	4.71	2.91	2.10	2.27	0.23	-	3.12	-
4h	4	5.10	2.26	2.63	1.23	0.54	0.55	-	0.60	-
8h	4	3.69	1.65	1.78	1.35	0.41	0.60	-	0.42	-
12h	4	2.82	1.29	1.42	1.12	0.34	0.55	-	0.32	-
16h	4	2.42	1.09	1.21	1.05	0.29	0.47	-	0.27	-
20h	4	2.24	0.95	1.11	1.06	0.26	0.46	-	0.24	-
24h	4	2.09	0.93	1.02	1.05	0.27	0.44	-	0.23	-
28h	4	1.98	0.88	0.97	1.01	0.26	0.40	-	0.23	-
32h	4	1.96	0.84	0.93	1.04	0.26	0.39	-	0.23	-
36h	4	1.90	0.80	0.88	1.02	0.25	0.37	-	0.22	-
40h	4	1.84	0.78	0.85	0.99	0.25	0.34	-	0.21	-
4h	6	1.11	0.30	0.48	0.50	0.13	0.37	-	<0.01	-
8h	6	0.87	0.25	0.43	0.58	0.11	0.35	-	<0.01	-
12h	6	0.75	0.28	0.44	0.56	0.13	0.39	-	<0.01	-
16h	6	0.68	0.26	0.41	0.53	0.12	0.35	-	<0.01	-
20h	6	0.62	0.26	0.39	0.51	0.12	0.31	-	<0.01	-
24h	6	0.60	0.25	0.38	0.50	0.12	0.29	-	<0.01	-
28h	6	0.57	0.25	0.36	0.49	0.12	0.27	-	<0.01	-
32h	6	0.53	0.25	0.34	0.47	0.12	0.25	-	<0.01	-
36h	6	0.52	0.24	0.33	0.45	0.12	0.24	-	<0.01	-
40h	6	0.51	0.23	0.32	0.45	0.11	0.22	-	<0.01	-

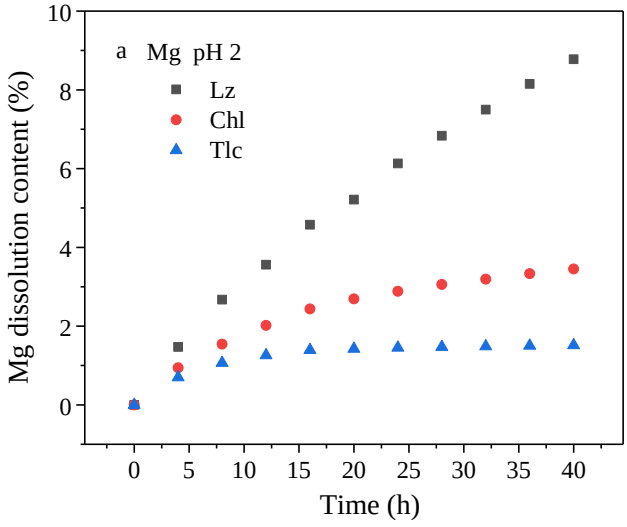

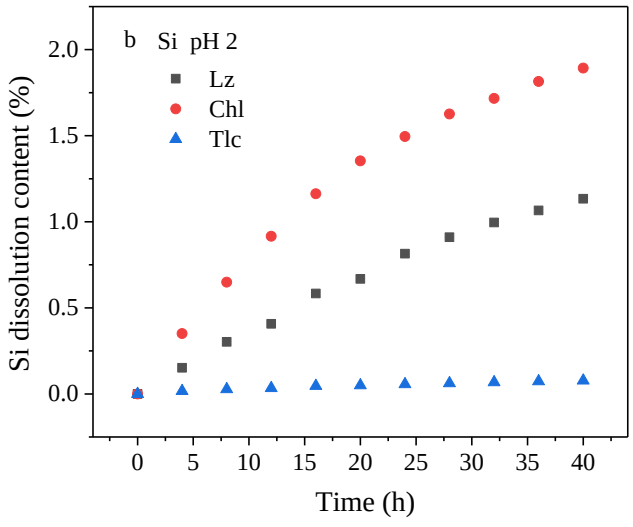

https://doi.org/10.1180/mgm.2024.57 Published online by Cambridge University Press

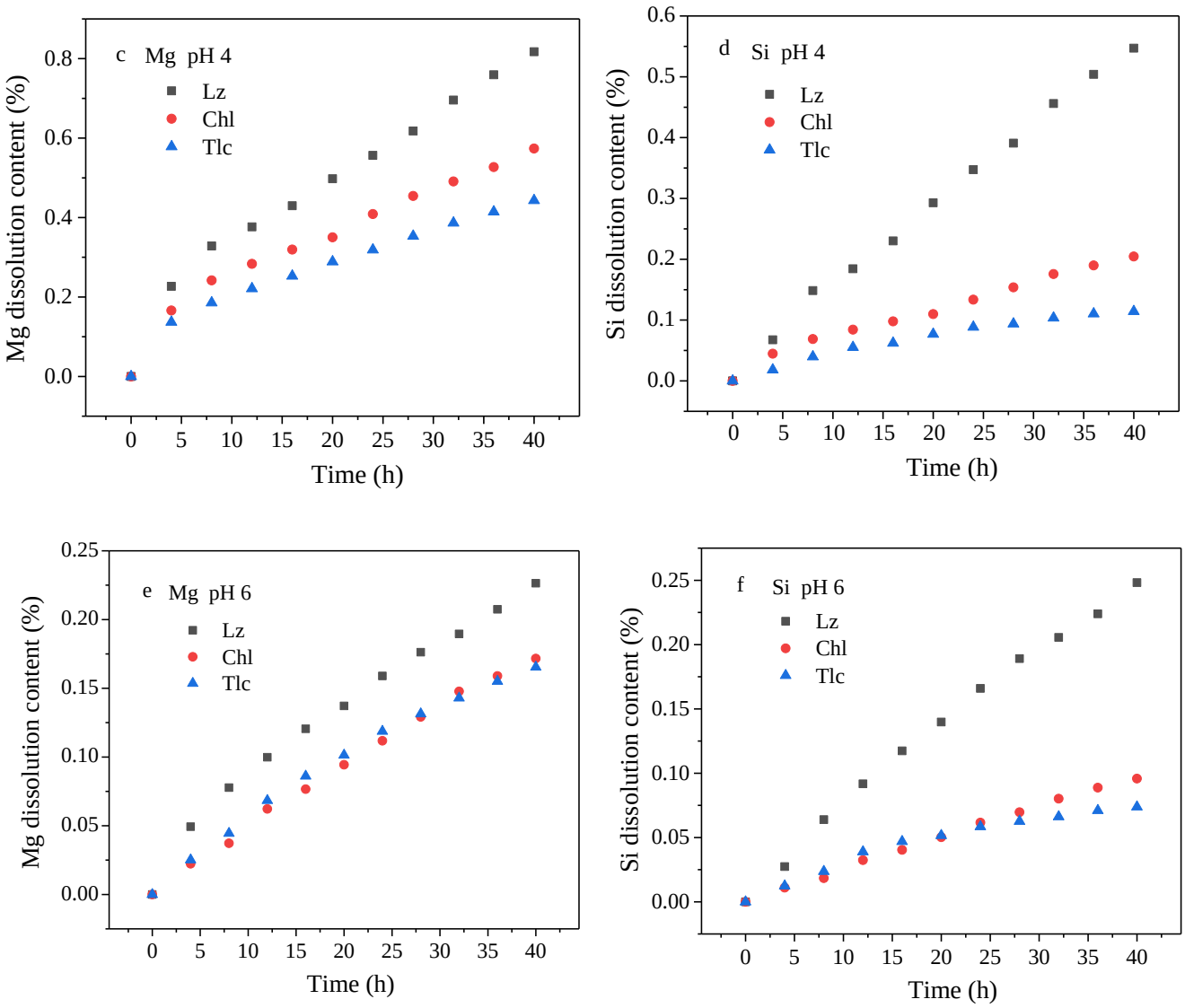

Fig.5. Effect of leaching time of sulfuric acid solution with pH values 2.0, 4.0 and 6.0 on dissolution efficiency of Mg and Si in minerals.

The concentration of Mg and Si in the filtrate collected each time was analyzed and calculated, and the dissolution efficiencies of Mg and Si in Lz, Chl and Tlc were obtained. In general, when sulfuric acid solutions with different pH values leached Lz, Chl and Tlc, the dissolution efficiencies of Mg and Si of the three minerals increased with the decrease of pH value. The dissolution efficiency of Mg in Lz is higher than that of Chl and Tlc under acidic pH values of 2.0, 4.0 and 6.0. The dissolution efficiency of Mg in Chl is greater than that of Tlc under acidic pH values of 2.0 and 4.0. When pH

https://doi.org/10.1180/mgm.2024.57 Published online by Cambridge University Press

value was 6.0, the dissolution efficiency of Mg in Chl and Tlc is basically the same (Fig. 5e). The difference in the dissolution efficiency of Mg is mainly due to the difference in the structure of minerals. Lz has a 1:1 type structure. When H^+ in sulfuric acid solution enters the interlayer domain, Mg-OH on each octahedral sheet reacts fully with H^+, and a large amount of Mg can be released from the octahedral sheet. While Tlc and Chl are 2:1 type structure minerals, H^+ attacks $(OH)^-$ on the octahedral sheets by the mineral edge (end surface), resulting in the destruction of the outer octahedral sheet and the dissolution of a small amount of Mg. When pH was 2.0, the dissolution efficiency of Mg in Lz gradually increases with the increase of leaching time, while the dissolution efficiency of Mg in Chl and Tlc increases first and then gradually approaches a constant value (Fig. 5a). In the early stage of the leaching process of Chl and Tlc, the dissolution of Mg is gradually carried out from the outside to the inside at the edge (end surface) (Saldi et al. 2007). Due to the dissolution of Mg, the silica tetrahedral sheets on both sides gradually collapse to the middle, resulting in the dissolution reaction between the solution and Mg-OH (Kameda et al. 2009). Therefore, the dissolution efficiency of 2:1 type minerals Mg is smaller than that of 1:1 type minerals, and the dissolution efficiency of Mg gradually stabilize after the first increase.

The differential dissolution of Mg in Chl and Tlc at pH values of 2.0 and 4.0 primarily occurs due to the structural differences between Chl and Tlc. In Chl, the interlayer domain consists of a brucite (Mg-OH) octahedral layer. The presence of H^+ ions can directly react with the brucite layer, leading to the destruction of the octahedral sandwich structure and subsequent dissolution of Mg from the Chl structure. The tetrahedral structure has the phenomenon that Al replaces Si, and Al occupies about 35% of the tetrahedral sheet. When Chl reacts with sulfuric acid solution, because the bond energy of Al-O bond is smaller than that of Si-O bond (Nnanwube et al. 2022, 2024), Al on tetrahedral

https://doi.org/10.1180/mgm.2024.57 Published online by Cambridge University Press

sheets will dissolve out before Si, resulting in defect sites on tetrahedral sheets. H^+ enters from these defect sites and reacts with octahedral sheets, increasing the dissolution efficiency of Mg. Due to the dissolution of Al from the mineral structure and subsequent hydrolysis reactions, it leads to the disruption of bridge oxygen between the tetrahedral and octahedral sheets, thereby expediting the dissolution process of both sheets (Bickmore et al., 2001; Li et al., 2020). The dissolution efficiency of Al is very important in the leaching process of Chl in acidic medium. This conclusion can be confirmed by Fig. 6. When the pH value is 2.0, Al/Si >1 (Fig. 6) during the mineral reaction, Al is preferentially dissolved from the tetrahedral sheet compared to Si. The dissolution efficiency of Mg in Chl is obviously higher than that of Tlc. When pH value is 4.0, Al/Si ≈ 1 during the reaction, indicating that the release amount of Al is equal to that of Si, and the dissolution efficiency of Al decreases, indicating that with the increase of pH value, the defect sites on tetrahedral sheets decrease, preventing H^+ from entering these defect sites and reacting with octahedral sheets. Therefore, the dissolution efficiency of Mg in Chl is slightly greater than that of Tlc. At pH 6.0, Al/Si ≈ 0 and remained constant during the reaction. This suggests that the dissolution efficacy of Al is negligible and can be disregarded. Consequently, the tetrahedral sheets exhibit a minimal number of defect sites during the water interface reaction process. Therefore, the dissolution efficiency of Mg in Chl is basically the same as that of Tlc.

At a pH of 2.0, the percentage of Si dissolution in chlorite is greater than that of Lz and Tlc (Fig. 5b) due to the preferential dissolution of Al in many tetrahedral sheets. (Hamer et al. 2003). As a result, Si is able to connect to the mineral surface through fewer than three bridging oxygen atoms, causing it to detach from the octahedral sheet more rapidly. Consequently, Si in Chl dissolves more easily compared to Lz and Tlc (Saldi et al. 2007).

https://doi.org/10.1180/mgm.2024.57 Published online by Cambridge University Press

The dissolution efficiency of Si in Lz is greater than that of Tlc, because there is a small amount of Al and Fe replacing Si in the silica tetrahedral sheet of Lz, while there is basically only Si on the tetrahedral sheet of Tlc, and there is almost no defect site, so the dissolution efficiency of Si in Tlc in the acid medium leaching process is the lowest. By comparing the dissolution efficiency of Si in Tlc when pH values are 2.0, 4.0 and 6.0, it can be found that the silicon-oxygen tetrahedron sheet in Tlc is very stable, and pH values have little or no effect on the dissolution efficiency of Tlc (Jurinski and Rimstidt, 2001). At pH values of 4.0 and 6.0, the dissolution efficiency of Si in Chl and Tlc is the same as that of Mg, which is related to the defect site on the tetrahedral sheet and controlled by the dissolution efficiency change of Al.

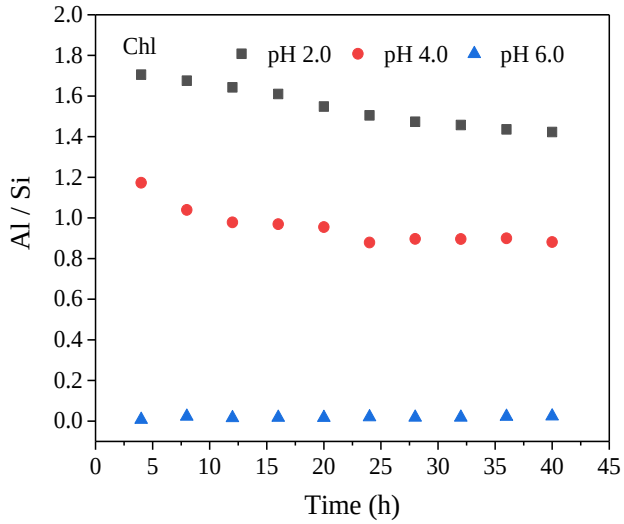

Fig.6. Effect of leaching time of sulfuric acid solution at pH 2.0, 4.0 and 6.0 on Al/ Si in Chl.

https://doi.org/10.1180/mgm.2024.57 Published online by Cambridge University Press

Mg/Si content variation in filtrate

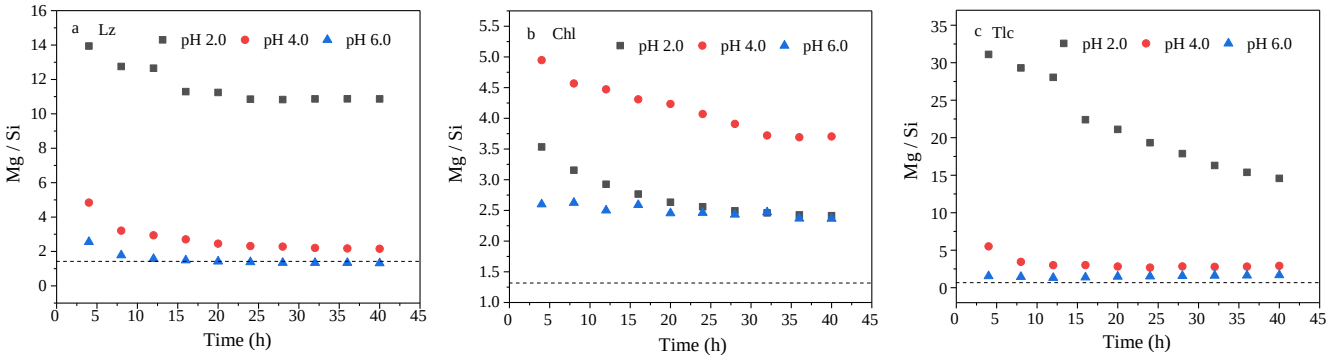

Fig.7. Effect of leaching time of sulfuric acid solution at different pH values on Mg/Si in filtrate of Lz, Chl and Tlc.

a. Lz; b. Chl; c. Tlc; The horizontal line represents the ideal stoichiometric ratio.

The sulfuric acid solutions with different pH values have great influence on Mg/Si ratio by leaching Lz, Chl and Tlc, and have different dissolution laws (Fig. 7). The general trend is that in acidic media with pH values of 2.0, 4.0 and 6.0, a gradual decrease in the Mg/Si ratio can be observed with increasing reaction time. This exponential dependence over time and the tendency to change in acidic media is consistent with other measurements of early silicate dissolution (Lin and Cemency, 1981; Schott and Berner, 1983, 1985).

With the increase of pH value, the Mg/Si ratio of Lz and Tlc is closer to the ideal stoichiometric ratio (Fig. 7a). Under the leaching of acidic medium with pH value of 6.0, the Mg/Si ratio of Lz gradually tends to be constant and reaches the ideal stoichiometric ratio with the progress of the reaction, and the Mg/Si ratio of Tlc is slightly higher than the ideal stoichiometric ratio. When pH value is 2.0, the Mg/Si dissolution ratio of the three minerals is as follows: Tlc > Lz > Chl. Because the tetrahedral sheet of Tlc is stable, and the tetrahedral sheet of Chl has the phenomenon of Al replacing Si, the reaction with H^+ will produce a large number of defect sites and lead to the dissolution of Si. The Mg/Si ratio of Chl at pH 4.0 is greater than that at pH 2.0 (Fig. 7b). This is

https://doi.org/10.1180/mgm.2024.57 Published online by Cambridge University Press

different from the dissolution rule of Mg/Si ratio of Lz and Tlc. This is because with the increase of pH value, the dissolution efficiency of Al in Chl greatly decreases, and the defect site on the tetrahedral sheet greatly decreases, resulting in the dissolution efficiency of Si also decreasing. It can be found that the change of Al dissolution efficiency in Chl will directly affect the size of Si dissolution efficiency, and the change of acidic pH value has a greater impact on the dissolution efficiency of Al.

Dissolution rate of Mg, Si and Al

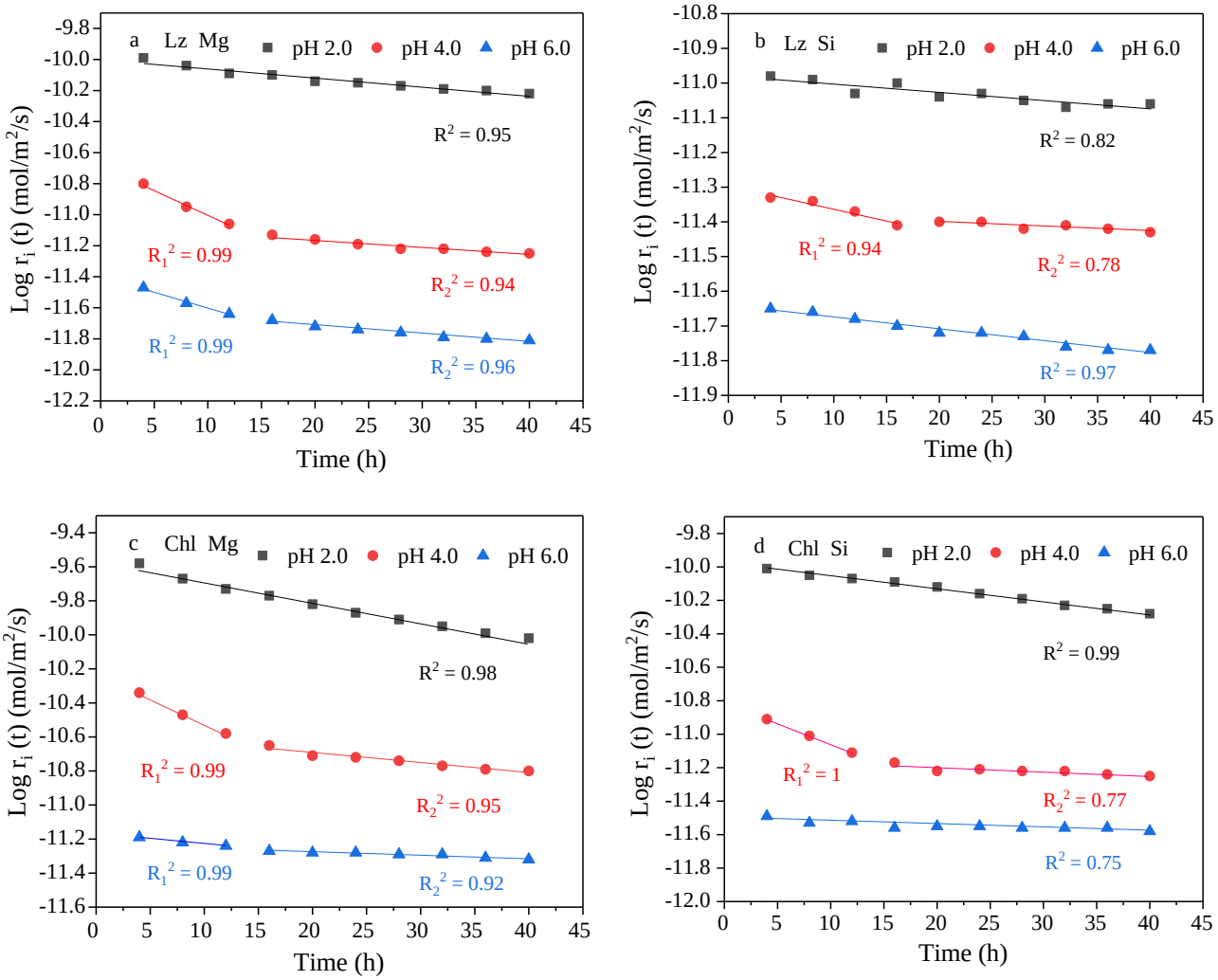

https://doi.org/10.1180/mgm.2024.57 Published online by Cambridge University Press

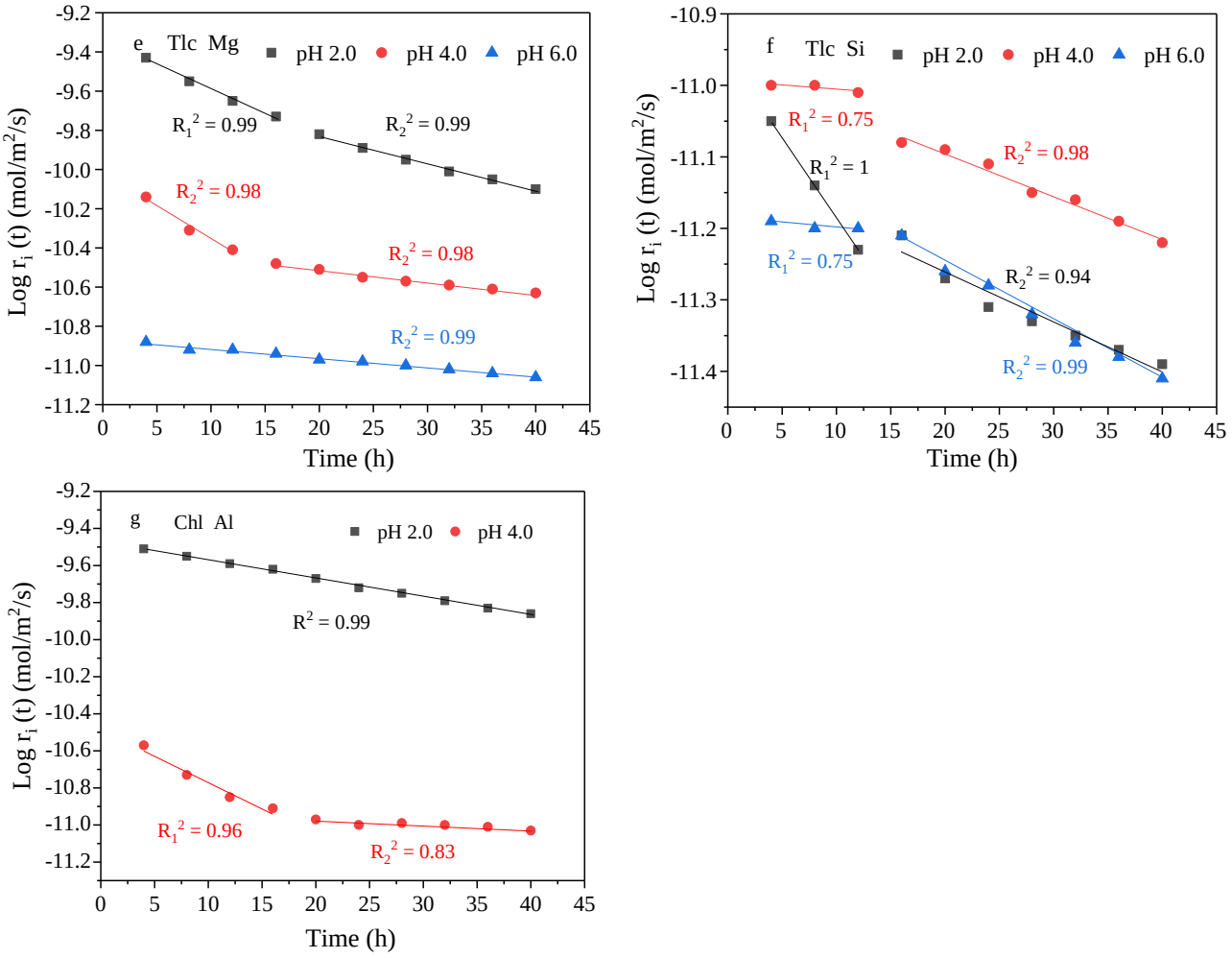

Fig.8. Effect of leaching time of sulfuric acid solution at different pH values on dissolution rate of Mg, Si and Al in Lz, Chl and Tlc (logarithmic form).

The normalisation of the reaction surface area is typically correlated with the macroscopic dissolving rate of ions in minerals. Various models for reaction surface area are proposed based on different minerals: (1) The reaction surface area is typically considered to be either the BET surface area of the mineral or directly proportionate to the BET surface area. (Ganor et al. 1999); (2) The reaction surface area is limited to certain crystal surfaces or is mainly controlled by surface defects (Nagy, 1995). When studying the dissolution kinetics of clay minerals, a common practice is to normalize the dissolution rate to their specific surface area (e.g., either partial or total surface including interlayer, external surface or edge surface; Bibi et al. 2011; Daval et al. 2013). Fig. 8 shows

https://doi.org/10.1180/mgm.2024.57 Published online by Cambridge University Press

the dissolution rates of Mg, Si and Al in acidic media with different pH values using BET surface area as the reaction surface area. The BET specific surface area test results were 17.8 m^2/g for Lz, 4.1 m^2/g for Chl, and 3.5 m^2/g for Tlc.

Although there are differences in mineral composition, such as the highest Mg content in Lz and the highest Si content in Tlc, the results of the study showed that the dissolution rate of minerals has a similar relationship with time and pH of the medium. In general, the dissolution rate of Mg and Si in Lz, Chl and Tlc decreased with the increase of time when pH values were kept at 2.0, 4.0 and 6.0. This may be due to the dissolution of fine particles and the preferential reaction of high surface activation energy regions or defect sites on large granular minerals during the initial phase of dissolution. For 2:1 type minerals (Chl and Tlc), the initial dissolution rate was higher, and the dissolution rate of Mg was higher than that of Si, due to the rapid ion exchange reaction between H^+ in the acidic medium and Mg in the outer layer of the octahedral sheet (Kohler et al. 2005; Bibi et al. 2011). Due to the high surface area of Lz, the dissolution rate of Mg is always lower than that of Chl and Tlc after normalization.

When the pH value is 2.0, the dissolution rate of Mg in Tlc presents a two-stage linear decrease trend during the reaction, which is different from the dissolution rate of Mg in Lz and Chl. The reason is that the dissolution of Mg in Tlc gradually proceeds from the outside to the inside at the edge (outer surface) during the reaction. Due to the dissolution of Mg, the silica tetrahedral sheet on both sides gradually collapses to the middle. As a result, the dissolution reaction between the solution and Mg-OH is blocked, so the dissolution rate of Mg gradually decreases. When pH value is 4.0, the dissolution rate of Lz, Chl and Tlc, Mg has a rapid decrease stage in the first 12 hours, and then the dissolution rate of Mg gradually decreases, showing a linear decrease trend in two stages during the

https://doi.org/10.1180/mgm.2024.57 Published online by Cambridge University Press

reaction. It can be found that the dissolution rate of Lz and Chl Mg is greatly affected by the increase of pH, that is, the dissolution of Lz and Chl are more sensitive to pH. The dissolution rate of Si in Lz and Chl has the same dissolution law in acidic media with different pH values, while the dissolution rate of Si in Tlc is almost unaffected by pH values (Jurinski and Rimstidt, 2001). At pH 2.0 and 4.0, the dissolution laws of Al (Fig. 8g), Mg and Si in Chl are the same (When pH value is 6.0, the dissolution of Al in Chl was found negligible).

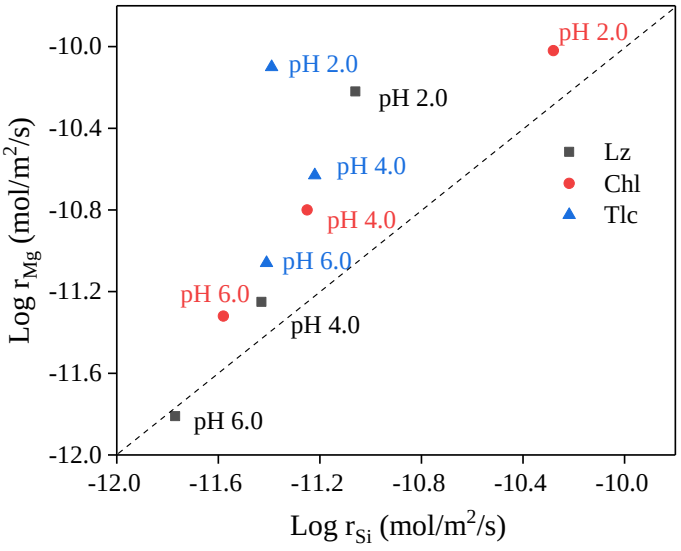

Fig.9. The logarithm of the dissolution rates of Mg and Si compared in sulfuric acid solutions of different pH values (the diagonal line corresponds to equal dissolution).

Previous studies on the dissolution reactions of 1:1 type and 2:1 type layered silicates in acidic media showed that cations in octahedral sheets were more easily released into solution than those in tetrahedral sheets (Kalinowski and Schweda, 2007; Rozalen et al. 2008; Krupskaya et al. 2017; Li et al. 2022). The reason is that the Mg-O bond is more likely to break than the Si-O bond, that is, the dissolution efficiency and dissolution rate of Mg in the octahedral sheet are greater than that of Si in the tetrahedral sheet. The dissolution laws of Lz, Chl and Tlc in acidic media in this paper are consistent with previous studies.

https://doi.org/10.1180/mgm.2024.57 Published online by Cambridge University Press

Model study on dissolution rate of Mg and Si

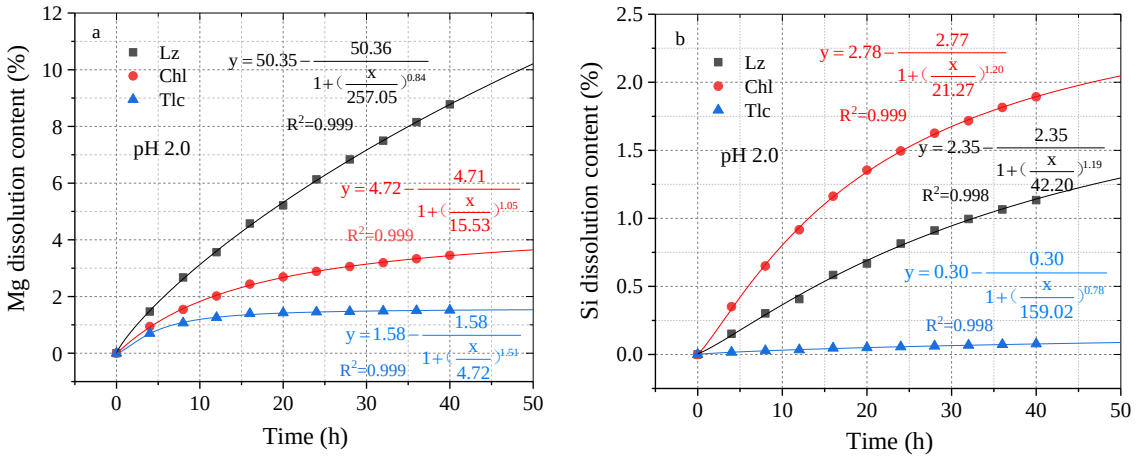

Fig.10. Logistic model was used to simulate the influence of sulfuric acid leaching time at pH value of 2.0 on the dissolution efficiency of Mg and Si in Lz, Chl and Tlc.

The dissolution efficiencies of Mg and Si in Lz, Chl, and Tlc were simulated using an open mineral-water interface reaction system. The simulations were conducted at a pH value of 2.0, and various models were compared. Ultimately, it was determined that the Logistic model effectively replicated the variations in dissolving percentages of Mg and Si in the three minerals as time progressed. The applicability of the Logistic function to investigations relating to clay minerals has been confirmed (Zhang et al. 2013; Chassagne, 2021; Chassagne and Safar, 2020; Ali and Chassagne, 2022). The Logistic function accurately fits the curve and shows strong agreement with the experimental values ($R^2 \geq 0.998$). The formula derived from curve fitting can be used to compute the dissolving percentages of Mg and Si in Lz, Chl, and Tlc at various reaction durations. Furthermore, it can also forecast the highest levels of dissolution for Mg and Si among the three minerals when exposed to sulfuric acid solution with a pH value of 2.0. As an illustration, Lz attains a condition of equilibrium when the proportion of Mg that dissolves is precisely 50.35%. Chl and Tlc, both belonging to the 2:1 type minerals, have maximum solubility percentages of Mg of just 4.72% and

https://doi.org/10.1180/mgm.2024.57 Published online by Cambridge University Press

1.58% respectively. These percentages are significantly lower than those of 1:1 type Lz. The maximum dissolution efficiency of Si in Lz, Chl and Tlc is less than Mg, and the difference of the maximum dissolution efficiency of Si in different layer structure minerals is small. The Si in Tlc exhibits exceptional stability, with a maximum dissolution efficiency of merely 0.30%. At pH values of 4.0 and 6.0, the concentration of H^+ ions are low and the reaction time is short. As a result, at the first stage of the dissolving process of Mg and Si in minerals, there is no suitable condition for establishing a model. Therefore, this study only established a model to simulate the dissolution efficiencies of Mg and Si in Lz, Chl and Tlc at a pH value of 2.0.

The investigation of the reaction kinetics model of Lz, Chl, and Tlc can directly illuminate the chemical reaction process of the mineral-water interface in an acidic medium and contribute to a better understanding of the mechanism of interaction between the two interfaces. In addition to forecasting the next experimental studies, the model's development can offer theoretical direction for the ion dissolution and migration of minerals in the aqueous media.

Conclusion

The leaching studies demonstrated that the pH values and reaction time have a significant impact on both the dissolution efficiencies and dissolution rates of Lz, Chl, and Tlc. Furthermore, they also result in the differential dissolution of Mg and Si components. The dissolution efficiency of Mg in Lz is higher than that of Chl and Tlc in acidic environment with pH values of 2.0,4.0 and 6.0. The dissolution efficiency of Mg in Chl is greater than that of Tlc in acidic environment with pH values of 2.0 and 4.0. At pH value of 6.0, the dissolution efficiency of Mg in Chl and Tlc is basically the same. This phenomenon is related to the defect site on the tetrahedral sheet of Chl and is controlled by the

https://doi.org/10.1180/mgm.2024.57 Published online by Cambridge University Press

change of the dissolution efficiency of Al.

The dissolution of Lz, Chl, and Tlc in sulfuric acid solution with varying pH values significantly affects the Mg/Si ratio and the speeds at which Mg and Si dissolve, and follows distinct dissolving patterns. The general trend is that the Mg/Si ratio can be observed to decrease gradually with the increase of reaction time in acidic media with pH of 2.0, 4.0 and 6.0. The Mg/Si ratio of Lz and Tlc is closer to the ideal stoichiometric ratio with the increase of pH. The dissolution rates of Si and Mg in Lz, Chl and Tlc decrease with the increase of reaction time in acidic medium with pH values of 2.0, 4.0 and 6.0, and there are two linear dissolution trends at different pH values. One reason is the dissolution of fine particles and the preferential reaction of high surface activation energy regions or defect sites on large-particle minerals, and the other reason is the structural difference between 1:1 type minerals and 2:1 type minerals. That is, the rapid ion exchange reaction between H^+ in the acidic medium and Mg located in the outer layer of the octahedral sheet of 2:1 type minerals.

A model was established to simulate and forecast the dissolution efficiencies of Mg and Si in Lz, Chl, and Tlc. The highest dissolving percentages of Chl and Tlc as 2:1 type minerals are determined to be only 4.72% and 1.58%, respectively. These values are significantly lower than the dissolution efficiency of 1:1 type Lz.

Acknowledgements. This study was supported by the National Natural Science Foundation of China (Grant No. 42072048).

Competing interests. The authors declare none.

https://doi.org/10.1180/mgm.2024.57 Published online by Cambridge University Press

References

Ali W. and Chassagne C. (2022) Comparison between two analytical models to study the flocculation of mineral clay by polyelectrolytes, *Continental Shelf Research*, **250**, 104864, ISSN 0278-4343, https://doi.org/10.1016/j.csr.2022.104864.

Amram K. and Ganor J. (2005) The combined effect of pH and temperature on smectite dissolute rate under acidic conditions. *Geochim Cosmochimica Acta*, **69**, 2535-2546.

Barnhisel R.I. and Bertsch P.M. (1989) Chlorites and hydroxy interlayered vermiculite and smectite. In: Dixon, J., Weed, S. (Eds.), *Minerals in Soil Environments*. Soc. Am pp. 729-788. https://doi.org/10.2136/sssabookser1.2ed.c15.

Brigatti M.F., Galan E. and Theng B.K.G. (2013) Structure and mineralogy of clay minerals. *In: Developments in Clay Science*, **5**, 21-81.

Bibi I., Singh B. and Silvester E. (2011) Dissolution of illite in saline-acidic solutions at 25 °C. *Geochim Cosmochim. Acta*, **75**, 3237-3249.

Bickmore B.R., Bosbach D., Hochella Jr M.F., Charlet L., and Rufe E. (2001) In situ atomic force microscopy study of hectorite and nontronite dissolution: Implications for phyllosilicate edge surface structures and dissolution mechanisms. *American Mineralogist*, **86**(4), 411-423.

Cappelli C., Yokoyama S., Cama J. and Huertas F.J. (2018). Montmorillonite dissolution kinetics: Experimental and reactive transport modeling interpretation. *Geochimica et Cosmochimica Acta*, **227**, 96-122.

Chassagne C. and Safar Z. (2020) Modelling flocculation: Towards an integration in large-scale sediment transport models. *Mar. Geol*, **430,** 106361.

Chassagne C. (2021) A simple model to study the flocculation of suspensions over time. *Chem. Eng. Res. Des*, **172**, 302-311.

Daval D., Hellmann R., Saldi G.D., Wirth R. and Knauss K.G. (2013) Linking nm-scale measurements of the anisotropy of silicate surface reactivity to macroscopic dissolution rate laws: New insights based on diopside. *Geochim. Cosmochim. Acta*, **107**, 121-134.

Douillard J.M., Salles F., Henry M., Malandrini H. and Clauss F. (2007) Surface energy of talc and chlorite: Comparison between electronegativity calculation and immersion results. *Journal of colloid and interface science*, **305**(2), 352-360.

https://doi.org/10.1180/mgm.2024.57 Published online by Cambridge University Press

Evans B.W., Hattori K. and Baronnet A. (2013) Serpentinite: what, why, where? *Elements*, **9**, 99-106. https://doi.org/10.2113/gselements.9.2.99.

Fuchs Y., Linares J. and Mellini M. (1998) Mossbauer and infrared spectrometry of lizardite-1T from Monte Fico, El ba. *Phys Chem Miner*, **26** (2):111-115. https://doi.org/10.1007/s002690050167.

Gazze S.A., Stack A.G., Ragnarsdottir K.V. and Mcmaster T.J. (2014) Chlorite topography and dissolution of the inte rlayer studied with atomic force microscopy. *Am Mineral*, **99** (1):128-138. https://doi.org/10.2138/am.2014.447 8.

Ganor J., Mogollon J.L. and Lasaga A.C. (1999) Kinetics of gibbsite dissolution under low ionic strength conditions. *Geochim Cosmochimica Acta*, **63**(11–12):1635–1651. https://doi.org/10.1016/S0016-7037(99)00069-1.

Golubev S.V., Bauer A. and Pokrovsky O.S. (2006) Effect of pH and organic ligands on the kinetics of smectite dissolution at 25°C. *Geochim Cosmochimica Acta*, **70**, 4436-4451.

Hamer M., Graham R.C., Amrhein C. and Bozhilov K.N. (2003) Dissolution of ripidolite (Mg, Fe-chlorite) in organic and inorganic acid solutions. *Soil Science Society of America Journal*, **67**(2), 654-661.

Hao W.D., Shannon L.F. and Teruhiko K. (2019) The impact of ionic strength on the proton reactivity of clay mineral. *Chemical Geology*, 529:119294.

He Z.Y., Zhang Z.Y., Yu J.X., Xu Z.G. and Chi R.A. (2016) Process optimization of rare earth and aluminum leaching from weathered crust elution-deposited rare earth ore with compound ammonium salts. *Rare Earths*, **34**,413-419. https://doi.org/10.1016/S1002-0721(16)60042-X.

Hegyesi N., Pongráccz S., Vad R.T. and Pukánszky B. (2020) Coupling of PMMA to the surface of a layered silicate by intercalative polymerization: processes, structure and properties. *Colloids and Surfaces A: Physicochemical and Engineering Aspects*, 601:12497. https://doi.org/10.1016/j.colsurfa.2020.124979.

Ikechukwu A.N, Mabel K. and Okechukwu D.O. (2022) Assessment of Owhe kaolinite as potential alumin-ium source in hydrochloric acid and hydrogen peroxide solutions: Kinetics modeling and optimization. *Cleaner Chemical Engineering*, **2**, 100022, ISSN 2772-7823, https://doi.org/10.1016/j.clce.2022.100022.

Ikechukwu A.N, Mabel K. and Okechukwu D.O. (2024) Kinetics of Owhe kaolinite leaching for alumina recovery in hydrochloric acid solution. *Scientific African*, **23**, e02045, ISSN 2468-2276, https://doi.org/10.1016/j.sciaf.202 3.e02045.

Jurinski, J.B. and Rimstidt, J.D. (2001) Biodurability of talc. *Am. Miner*, **86**, 392-399.

Kalinowski, B.E. and Schweda, P. (2007) Rates and nonstoichiometry of vermiculite dissolution at 22 °C. *Geoderma*,

https://doi.org/10.1180/mgm.2024.57 Published online by Cambridge University Press

142, 197-209.

Kameda J., Sugimori H. and Murakami T. (2009) Modification to the crystal structure of chlorite during early stages of its dissolution. *Physics and Chemistry of Minerals*, **36**: 537-544.

Kalinowski B.E. and Schweda P. (1996) Kinetics of muscovite, phlogopite and biotite dissolution and alteration at pH 1 to 4, room temperature. *Geochim Cosmochimica Acta*, **60**, 367-385.

Kohler S.J., Bosbach D. and Oelkers E.H. (2005) Do clay mineral dissolution rates reach steady state? *Geochim. Cosmochim. Acta*, **69**, 1997-2006.

Krupskaya V.V., Zakusin S.V., Tyupina E.A., Dorzhieva O.V., Zhukhlistov A.P., Belousov P.E., and Timofeeva M.N. (2017) Experimental study of montmorillonite structure and transformation of its properties under treatment wit h inorganic acid solutions. *Minerals*, **7**(4), 49.

Krupskaya V.V., Novikova L., Tyupina E., Belousov P., Dorzhieva O., Zakusin S., and Belchinskaya L. (2019) The in fluence of acid modification on the structure of montmorillonites and surface properties of bentonites. *Applied Clay Science*, **172**, 1-10.

Lacinska A.M., Styles M.T., Bateman K., Wagner D., Hall M.R., Gowing C. and Paul D.B. (2016) Acid-dissolution o f antigorite, chrysotile and lizardite for ex situ carbon capture and storage by mineraliz-ation. *Chemical Geology*, **437**, 153-169. https://doi:10.1016/j.chemgeo.2016.05.015.

Li S., He H., Tao Q., Zhu J., Tan W., Ji S., and Zhang C. (2020) Kaolinization of 2:1 type clay minerals with different swelling properties. *American Mineralogist*, **105**(5), 687-696.

Li K.W., Lu H.L., Nkoh J.N., Hong Z.N. and Xu R.K. (2022) Aluminum mobilization as influenced by soil organic matter during soil and mineral acidification: A constant pH study. *Geoderma*, **418**, 115853.

Liao R., Chen W., Wang N. and Zhang J. (2021) Combined effects of temperature, mineral type, and surface roughness on chlorite dissolution kinetics in the acidic pH. *Applied Clay Science*, **201**, 105931.

Lin F.C. and Cemency C.V. (1981) The dissolution kinetics of brucite, antigorite, talc and phlogopite at room temperature and pressure. *Am. Min*, **66**, 801-806.

Lin S.M., Yu Y.L., Zhang Z.J., Zhang C.Y., Zhong M.F., Wang L.M. and Huang X. (2020) The synergistic mechanisms of citric acid and oxalic acid on the rapid dissolution of kaolinite. *Applied Clay Science*, **196**, 105756.

Malmström M. and Banwart S. (1997) Biotite dissolution at 25°C: the pH dependence of dissolution rate and stoichiometry. *Geochim Cosmochimica Acta*, **61**, 2779-2799.

https://doi.org/10.1180/mgm.2024.57 Published online by Cambridge University Press

Meng P., Li Z., Huang Z., and Chen C. (2016) Extraction of potassium from biotite by Ba^{2+}/K^{+} ion exchange and the structural transformation. *Physics and chemistry of minerals*, **43**, 387-393.

Mellini M. and Zanazzi P.F. (1987) Crystal structures of lizardite 1T and lizardite-2H1 from Coli, Italy. *Am Mineral*, **72** (9–10):943–948.

Nagy K.L. (1995) Dissolution and precipitation kinetics of sheet silicates. *Reviews in Mineralogy and Geochemistry*, **31**(1):173-233.

Nnanwube I.A., Keke M. and Onukwuli O.D. (2022) Assessment of Owhe kaolinite as potential aluminium source in hydrochloric acid and hydrogen peroxide solutions: kinetics modeling and optimization. *Cleaner Chemical Engineering*, **2**, 100022.

Nnanwube I. A., Keke M. and Onukwuli, O.D. (2024) Kinetics of Owhe kaolinite leaching for alumina recovery in hydrochloric acid solution. *Scientific African*, **23**, e02045.

Peng C., Min F., Liu L., and Chen J. (2016) A periodic DFT study of adsorption of water on sodium-montmorillonite (001) basal and (010) edge surface. *Applied Surface Science*, **387**, 308-316.

Ren Y., Cao X. and Wu P. (2023) Experimental insights into the formation of secondary minerals in acid mine drainage-polluted karst rivers and their effects on element migration. *Science of The Total Environment*, 858: 160076.

Ross G.J. (1969) Acid dissolution of chlorites: Release of Magnesium, Iron and Aluminum and mode of acid attack. *Clays and Clay Mineral*, **17**, 347-354.

Rozalen M.L., Huertas F.J., Brady P.V., Cama J., Garcia-Palma S. and Linares J. (2008) Experimental study of the effect of pH on the kinetics of montmorillonite dissolution at 25 °C. *Geochim. Cosmochim. Acta*, **72**, 4224-4253.

Saldi G.D., Köhler S.J., Marty N. and Oelkers E.H. (2007) Dissolution rates of talc as a function of solution composition, pH and temperature. *Geochim cosmochimica acta*, **71**(14), 3446-3457.

Schott J. and Berner R.A. (1983) X-ray photoelectron studies of the mechanism of iron silicate dissolution during weathering. *Geochim. Cosmochim. Acta*, **47**, 2233-2240.

Schott J. and Berner R.A. (1985) Dissolution mechanism of pyroxenes and olivines during weathering. In: Drever, J.I. (Ed.), *The Chemistry of Weathering*, **149**. Reidel, Dordrecht.

Sposito G. (1989) The Chemistry of Soils. Oxford University Press.

Stumm W. and Wieland E., 1990. Dissolution of oxide and silicate minerals: rates depend on surface speciation. In: Stumm, W. (Ed.), *Aquatic Chemical Kinetics*, Wiley, pp. 367-400.

https://doi.org/10.1180/mgm.2024.57 Published online by Cambridge University Press

Turpault M.P. and Trotignon L. (1994) The dissolution of biotite single crystals in dilute HNO_3 at 24°C Evidence of an anisotropic corrosion process of micas in acidic solutions. *Geochim Cosmochimica Acta*, **58**, 2761-2775.

Wang L., Lu A., Wang C., Zheng X., Zhao D. and Liu R. (2006) Nano-fibriform production of silica from natural chr ysotile. *Journal of colloid and interface science*, **295**(2), 436-439.

Zhang X.C, Chen W.P., Ma C. and Zhan S.F. (2013) Modeling particulate matter emissions during mineral loading pr ocess under weak wind simulation, *Science of The Total Environment*, **449**, 168-173, ISSN 0048-9697, https://d oi.org/10.1016/j.scitotenv.2013.01.050.

https://doi.org/10.1180/mgm.2024.57 Published online by Cambridge University Press